EMC improvement of a DC-DC boost converter

Author: Max Helmich and Kilian Makswit

1 Introduction

This documentation presents a solution to the optimization of a DC-DC boost converter facing EMC problems in the context of the IEEE Student Contest 2022. Given is a LTspice model of the converter (depicted in figure 1) and design specifications which need to be met. The snubber elements, the MOSFET's gate resistance, and the switching operation have to be adjusted to minimize the maximum output voltage to steady state level ratio. In addition, a minimum efficiency of 92% and a steady state output voltage of $47 - 49$ V are to be achieved.

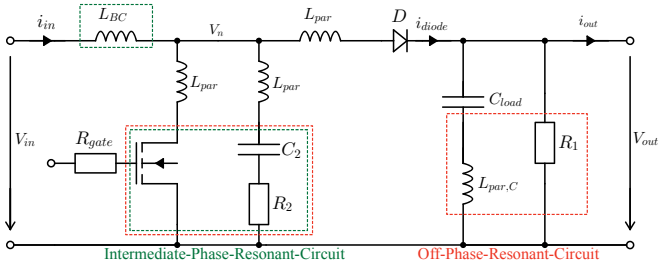

Figure 1: Given DC-DC Boost Converter Architecture.

2 Resonant Circuit Identification

For poorly tuned element parameters several oscillation phenomena can be observed during the boost-converter operation (see figure 2).

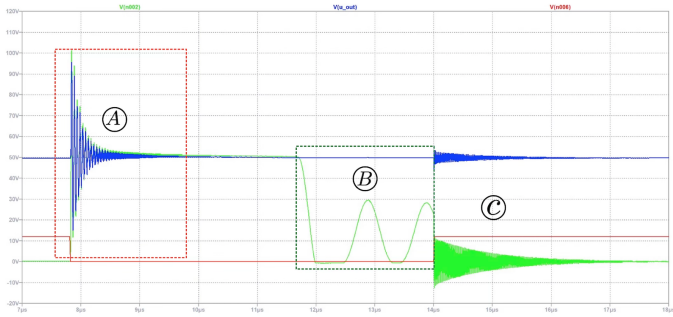

Figure 2: Boost Converter Characteristic with Poorly Tuned Element Values - Blue: Output Voltage, Green: V_n Potential, Red: MOSFET's Switching Signal.

Oscillation A is caused by switching the MOSFET off. The potential V_n (see figure 1) oscillates around a mean value which is given by the output voltage V_{out} reduced by the Schottky diode diffusion voltage V_{diode}. This oscillation is mainly determined by a fundamental oscillation which involves the Off-Phase-Resonant-Circuit (see figure 1). Further, higher harmonics caused by parasitic inductive and capacitive elements superimpose.

During oscillation B energy is exchanged between the inductive and capacitive elements of the Intermediate-Phase-Resonant-Circuit (see figure 1). The mean value of this oscillation is given by the input voltage level. Note, that the oscillation cannot exceed the bulk-drain pn-junction diffusion voltage of the MOSFET around $-0.7V$ which is why plateaus appear in the output plot.

Oscillation C is related to switching-on the MOSFET and its amplitude depends on the initial V_n potential before it is pulled to ground. The parasitic inductances and the Schottky diode's diffusion capacitance are mainly involved.

3 EMC-Improvement of Boost-Converter Design

This section aims at finding suitable mathematical descriptions to approximate the physical behaviour of occurring effects. This is essential for knowing exactly how the given parameters must be adjusted to come to an effective design.

3.1 Off-Phase-Resonant-Circuit

In the following subsection we neglect the higher order harmonics to encounter dominant effects associated with the fundamental oscillation. As oscillation A is directly coupled to the output it strongly influences the output voltage to steady state level ratio. Therefore, the peak-overshoot must be reduced.

The Off-Phase-Resonant-Circuit can be represented by the equivalent circuit illustrated in figure 3.

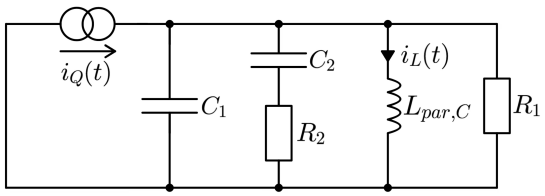

Figure 3: Equivalent Off-Phase-Resonant-Circuit.

The MOSFET's parasitic capacitance is represented by C_1 in the Off-Phase-Condition. It was determined by analysing the eigenfrequency of the resonance circuit. As the output capacitance value is much larger than the other involved capacitances, it can be neglected. The Schottky diode does not appear in the equivalent circuit. When a certain current is provided by the input inductor, the current which is not sunk by the output elements is forced in the first part of the resonant circuit allowing an oscillation, even though the diode current does not change direction.

A general excitation of the equivalent resonant circuit can be described by the current source $i_Q(t)$. The circuit's dynamic behaviour is described by the following differential equation:

$$\begin{aligned} &\underbrace{\frac{1}{C_1 L_{BC}}}_{b_1}\frac{di_Q}{dt} + \underbrace{\frac{1}{C_1 C_2 R_2 L_{BC}}}_{b_0} i_Q = \\ &\frac{d^3 i_L}{dt^3} + \underbrace{\left[\frac{1}{R_2 C_1} + \frac{1}{R_2 C_2} + \frac{1}{R_1 C_1}\right]}_{a_2}\frac{d^2 i_L}{dt^2} + \\ &\underbrace{\left[\frac{1}{C_1 C_2 R_1 R_2} + \frac{1}{C_1 L_{BC}}\right]}_{a_1}\frac{di_L}{dt} + \underbrace{\frac{1}{C_1 C_2 R_2 L_{BC}}}_{a_0} i_L \end{aligned} \tag{1}$$

Using this equation, the transfer function of the system can be derived:

$$\frac{I_L}{I_Q} = \frac{b_1 s + b_0}{s^3 + a_2 s^2 + a_1 s + a_0} \tag{2}$$

To further investigate the oscillations, a 2nd order system reduction is suitable as oscillations can only be caused by two complex conjugated poles in the s-plane. Equation 3 shows the general form of a 2nd order system transfer function:

$$G(s) = \frac{w_0^2}{s^2 + 2\delta w_0 s + w_0^2} \tag{3}$$

From the pole locations one can extract the eigenfrequency ω and the damping $\delta = sin(\theta)$ (see figure 4).

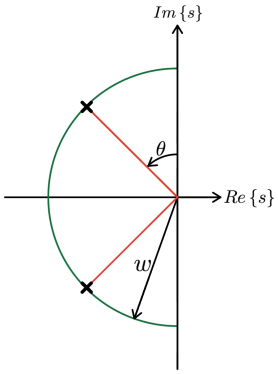

Figure 4: Pole Properties of a 2nd Order System.

When using the second order approximation, the relative peak overshoot is given by:

$$M_p = e^{-\frac{\pi\delta}{\sqrt{1-\delta^2}}} \tag{4}$$

This relationship shows that the damping of the system should be chosen to be one, corresponding to poles located on the negative real axis of the s-plane. To achieve this design objective, a developed MATLAB code extracts the eigenfrequency w and the damping δ for different values of the snubber resistance R_2 and a fixed snubber capacitance C_2. The simulation results provide a range in which R_2 can be chosen ensuring $\delta = 1$ (see figure 5).

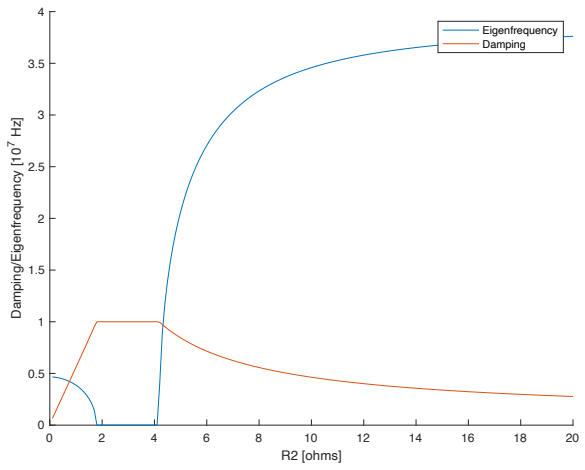

Figure 5: Damping and Eigenfrequency Curve for $C_2 = 38nF$.

Taking into account the 3rd order behaviour of the resonant circuit to verify the 2nd order approximation, a step response was applied to the 3rd order system. It could be observed that the 2nd order approximation described the damping range very well. However, it turned out that the 3rd order system showed strongly damped overshoots even for $\delta = 1$. The overshoot is strongly influenced by the system's left-half-plane-zero. The influence of the zero can be minimized by achieving pole-zero compensation with the third pole. It can be shown that the pole and the zero approach each other for high C_2 values, which is why it is reasonable to choose latter to be as large as possible in our design.

3.2 Intermediate-Phase-Resonant-Circuit

To reduce the peak overshoot of oscillation C, to set the output voltage accordingly, and to find an upper limitation of C_2 the Intermediate-Phase-Resonant-Circuit is taken into consideration.

The Intermediate-Phase-Resonant-Circuit can be represented by the equivalent circuit illustrated in figure 6.

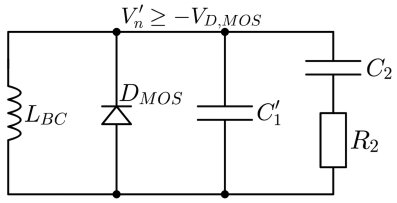

Figure 6: Equivalent Intermediate-Phase-Resonant-Circuit.

For the device operation we decided to include an intermediate phase to avoid a sudden drop of the V_n potential to ground, when the MOSFET is switched on. This drop would lead to a significant stimulation of oscillation C. Further, the period time was chosen in such a way that the MOSFET is switched on during times when the V_n' potential is at the negative pn-junction diffusion voltage $V_{D,MOS}$. This ensures a neglectable stimulation of the oscillation C such that no output ripple occurs at switching. To ensure high efficiency by avoiding losses during the oscillation over the resistive elements, we chose the switching event to occur during the first plateau.

Now a fixed switching pattern can be defined to find a mathematical representation of the whole switching cycle:

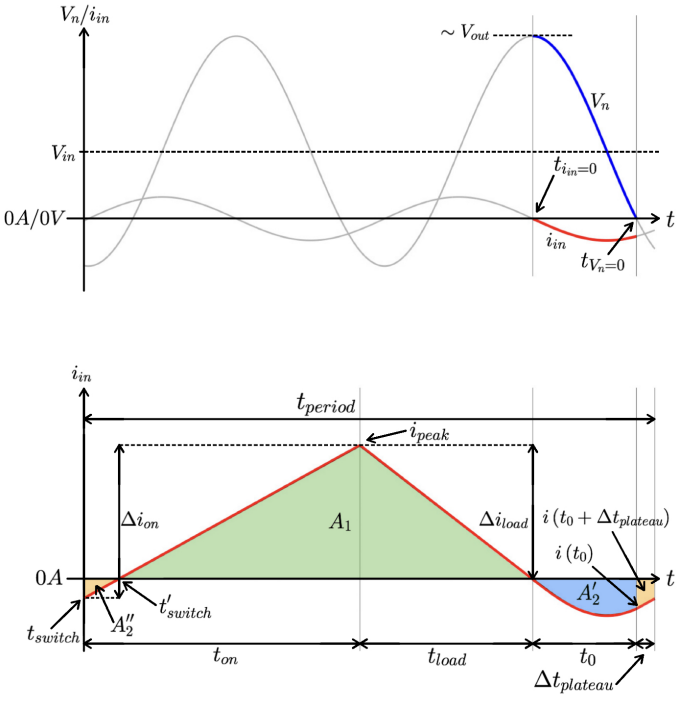

Figure 7: Inductor Current Curve During one Operation Cycle in Steady State. V_n and i_n are Phase-Shifted by 90° as they are Related by the L_{BC} Inductance.

The time t_0 is defined as the difference between $t_{V_n=0}$ when the V_n potential crosses 0 V and enters the plateau and $t_{I_{ind}=0}$ when the inductor current crosses 0 A and decouples the Schottky diode branch. The time $\Delta t_{plateau}$ is a design parameter which must be smaller than the total width of the plateau. The time t_{on} is the charge time of the inductor L_{BC} which will firstly be treated as fixed, but will be considered in efficiency considerations later. The time t_{load} describes the charge period of the output capacitance. Fixed L_{BC} charging and discharging slopes together with a fixed t_{on} define the peak current i_{peak}, which therefore only depends on the initial inductor current value at t_{switch}. Now the constant discharging slope implies a direct relation between i_{peak} and t_{load} making t_{load} only depending on $\Delta t_{plateau}$. Therefore, the time t_{period} comprises:

$$t_{period} = t_{on} + t_0 + t_{load}(\Delta t_{plateau}) + \Delta t_{plateau} \tag{5}$$

Taking this mathematical description as a basis, one can derive the following relation for the output voltage (see Appendix):

$$V_{out} = \frac{\frac{i_{peak}\Delta t_{load}}{2t_{period}}}{\frac{C_2}{2t_{period}} + \frac{1}{R_{out}}} \tag{6}$$

Now we are interested in finding the C_2 value for a given $\Delta t_{plateau}$ such that a defined output voltage is reached. To achieve this, V_{out} was set to a defined value of 47 V and the equation was solved numerically. This was done for multiple $\Delta t_{plateau}$ times to obtain all possible C_2 values.

In a second step, the maximum plateau width $t_{plateau}$ was calculated in dependence on the above calculated C_2 value range. This width depends on the eigenfrequency of the oscillation B and is given by:

$$t_{plateau} = \frac{2\pi}{w} - 2t_0 \tag{7}$$

This is the upper limit for applicable $t_{plateau}$ times to not stimulate oscillation C.

Plotting both curves provides the following graph:

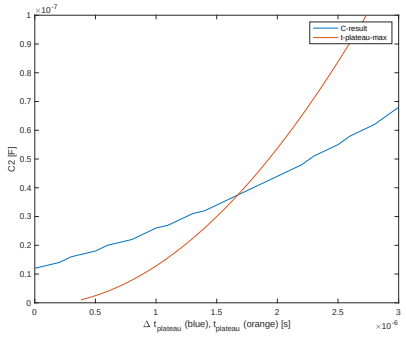

Figure 8: Optimimization Graph for C_2 Values.

As depicted in figure 8, the C_2 values can only be chosen in a certain range as $\Delta t_{plateau}$ must not be greater than $t_{plateau}$. Given the design objective in section 3.1, C_2 should be selected as large as possible to minimize overshoots in the output voltage characteristic. Consequently, C_2 was picked as the intersection of both curves.

4 Design Procedure

Using the developed mathematical models, the design algorithm depicted in figure 9 was developed to optimize the EMC performance of the boost converter.

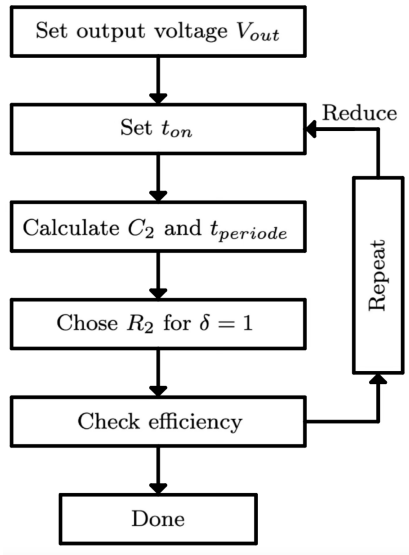

Figure 9: Steps Taken for EMC Optimization.

The algorithm contains efficiency optimisation which has not been considered yet. Assuming a fixed input voltage and a fixed output power, the efficiency only depends on the inductor current. Consequently, the efficiency is mainly related to the ration of $\frac{A1}{A2}$ in figure 7. In case of matching the t_{switch} time to the 0 A crossing, one can show that $A_1 \propto t_{on}^2$ and $A_2 \propto \sqrt{C_2}$ which is a good approximation to investigate the area ratio (see appendix). The C_2 optimization curves indicated that when reducing t_{on}, the snubber capacitance value C_2 must be decreased to obtain the same output voltage level. This is reasonable, as for decreasing t_{on} times a larger fraction of the available input current must directly be provided to the output load capacitance (to support the output voltage), instead of charging C_2. Therefore, an increase in efficiency can be achieved by reducing t_{on} as A_1 decreases faster than A_2. However, to small t_{on} values should be avoided as reducing C_2 results in higher overshoots.

Taking the higher harmonics back into account, they were removed by a sufficient choice of the MOSFET's input resistor R_{gate} and the previous choice of the snubber resistance R_2. As higher harmonic damping could easily be achieved without affecting the boost converter's performance, no further investigations regarding modelling and description of the harmonics have been conducted.

Finally, after having followed the provided design scheme the following design parameters were obtained:

Design Parameter	Value
t_{period}	19.0 μs
t_{on}	11.8 μs
R_2	3.6 Ω
C_2	37 nF
R_{gate}	20 Ω

Appendix

Derivation of the Output Voltage - Snubber Capacitance Relation

Using the convention in figure 7, the following relationships were used to come to an expression for the output voltage V_{out} in dependence of the snubber resistance C_2:

$$\Delta i_{on} = \frac{1}{L_{BC}} V_{in} t_{on} \tag{8}$$

$$t_0 = \arccos\left(\frac{-V_{in}}{Vout - V_{in}}\right)\frac{1}{w} \tag{9}$$

$$i(t_0) = \sqrt{\frac{C}{L_{BC}}[V_{out} - V_{in}]^2} * -\sin(wt_0) \tag{10}$$

$$i_{peak} = \Delta i_{load} \tag{11}$$

$$\Delta i_{load} = \frac{1}{L_{BC}}[V_{out} - V_{in}]t_{load} \tag{12}$$

$$i(t_0 + \Delta t_{plateau}) = i(t_0) + \frac{(V_{in} + V_{diode})\Delta t_{plateau}}{L_{BC}} \tag{13}$$

$$\Delta i_{load} = i(t_0 + \Delta t_{plateau}) + \Delta i_{on} \tag{14}$$

Using equations 11, 12, and 14 one can derive:

$$t_{load} = \frac{i(t_0 + \Delta t_{plateau}) + \Delta i_{on}}{V_{out} - Vin} L_{BC} \tag{15}$$

Now the quantities are being related to the output voltage V_{out} by a power balancing analysis:

$$P_{in} = P_{out} + P_{loss} \tag{16}$$

$$P_{in} = \frac{i_{peak}^2 \Delta t_{load}}{2} V_{out} \frac{1}{t_{period}} \tag{17}$$

$$P_{out} = \frac{V_{out}^2}{R_{out}} \tag{18}$$

$$P_{loss} = \frac{\Delta E_{loss}}{t_{period}} \tag{19}$$

The energy absorbed by the snubber elements over one period can be approximated by:

$$V_{C_2} = \left(1 - e^{-\frac{t}{C_2 R_2}}\right) V_{in} \tag{20}$$

$$i_{C_2}(t) = C_2 \frac{dV_{C_2}}{dt} \tag{21}$$

$$i_{C_2}(t) = \frac{1}{R_2} e^{-\frac{t}{R_2 C_2}} V_{in} \tag{22}$$

$$\Delta E_{loss} = \int_0^\infty i_{C_2}^2 R_2 dt = \int_0^\infty \frac{1}{R_2} e^{-\frac{2t}{R_2 C_2}} V_{in}^2 dt = \frac{V_{in}^2 C_2}{2} \tag{23}$$

Using the above formulas the output voltage can be expressed as:

$$V_{out} = \frac{\frac{i_{peak}\Delta t_{load}}{2t_{period}}}{\frac{C_2}{2t_{period}} + \frac{1}{R_{out}}} \tag{24}$$

Efficiency Evaluation

To find a compact relation for the area ratio $\frac{A_1}{A_2}$, the switching event t_{switch} is considered to happen at the 0 A crossing (see t'_{switch} in figure 7). Applying this case, the following relationships can be derived:

$$i_{peak} = \Delta i_{on} \tag{25}$$

$$t_{load} = \frac{\Delta i_{on}}{V_{out} - V_{in}} L_{BC} = \frac{V_{in} t_{on}}{V_{out} - V_{in}} \tag{26}$$

$$|A_1| = \frac{i_{peak}[t_{on} + t_{load}]}{2} = \frac{1}{2L_{BC}} V_{in} t_{on}^2 \left(1 + \frac{V_{in}}{V_{out} - V_{in}}\right) \tag{27}$$

$$A'_2 = \int_0^{t_0} i_{in}(t) dt = \sqrt{\frac{C_2}{L_{BC}[V_{out} - V_{in}]^2}}[\cos(wt_0) - 1] \tag{28}$$

$$|A_2| = |A'_2| + \left|\frac{i_{t0} t_{plateau}}{2}\right| = \sqrt{\frac{C_2}{L_{BC}[V_{out} - V_{in}]^2}} * \text{const.} \tag{29}$$

It can be observed that A_1 is proportional to t_{on}^2 and that A_2 is proportional to $\sqrt{C_2}$.